

Research Article

Study the Behavior of Drug Structures via Chemical Invariants Using TOPSIS and SAW

Salma Kanwal¹, Yasmeen Farooq,¹ Muhammad Kamran Siddiqui,² Nazeran Idrees³, Asima Razzaque⁴, and Fikre Bogale Petros⁵

¹Department of Mathematics, Lahore College for Women University, Lahore, Pakistan

²Department of Mathematics, COMSATS University Islamabad, Lahore Campus, Pakistan

³Department of Mathematics, Government College University, Faisalabad, Pakistan

⁴Basic Science Department, Preparatory Year Deanship, King Faisal University, Al Ahsa, Saudi Arabia

⁵Department of Mathematics, Addis Ababa University, Addis Ababa, Ethiopia

Correspondence should be addressed to Fikre Bogale Petros; fikre.bogale@aau.edu.et

Received 15 May 2022; Revised 1 July 2022; Accepted 24 November 2022; Published 30 January 2023

Academic Editor: Naeem Jan

Copyright © 2023 Salma Kanwal et al. This is an open access article distributed under the Creative Commons Attribution License, which permits unrestricted use, distribution, and reproduction in any medium, provided the original work is properly cited.

Every year, various experiments emerge in which a strong link between topological chemical structures and their properties is found. These properties are numerous such as melting point, boiling point, and drug toxicity. Topological index is the functional tool to determine these properties. This research paper will analyze some of the molecular drug structures, i.e., hyaluronic acid-paclitaxel conjugates G_n , anticancer drug SP[n], polyomino chain of n -cycle Z_n , triangular benzenoid T_n , and circumcoronene benzenoid series H_k using multicriteria decision-making techniques including TOPSIS and SAW. The topological indices used in this research paper include the Randić index for $\alpha = 1, -1, 1/2$, the augmented Zagreb index and the forgotten topological index.

1. Introduction

The introduction of mathematical “graph theory” to chemistry [1] has been playing a significant role. Chemical graph theory is a subset of graph theory that connects to chemical compounds and processes. Chemical graph theory depicts molecular structures as chemical graphs, with nodes and edges representing atoms and bonds. In cheminformatics, they depict chemical structures. The cornerstone for (quantitative) structure activity and structure property predictions—a key field of cheminformatics—is computable properties of graphs. These graphs can be reduced to descriptors or indices based on graph theory, which reflect the physical properties of molecules [2]. Topological indices are numerical values linked with chemical constitution that aim to link chemical structure to physical attributes, chemical reactivity, and biological activity. These distance-based graphical indices are commonly employed to build correlations between molecular graph structure and characteristics.

Chemical compounds’ physicochemical qualities and bioactivity can be predicted using topological indices [3]. Gao et al. [4] referred chemical and pharmaceutical processes to have advanced rapidly, resulting in the emergence of a slew of novel nanomaterials, crystals, and medications each year. The examination of these various chemicals necessitates a significant number of chemical experiments, which adds to researchers’ burden. According to Katritzky et al. [5], their experiments reveal a close link between topological molecule structures and their physical behaviors, chemical properties, and biological traits, such as melting point, boiling temperature, and drug toxicity. Any drug that is effective in the treatment of cancerous disease is known as an anticancer drug, also known as effective anticancer drug. Anticancer medications are divided into various categories, including alkylating agents, antimetabolites, natural compounds, and hormones. Additionally, there are a number of medications that do not fall into those classifications but have anticancer action and are thereby employed in the treatment of cancer.

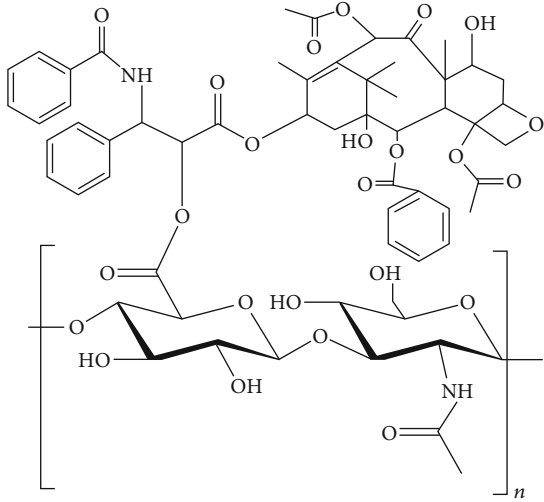


FIGURE 1: Molecular graph of HA-paclitaxel conjugates.

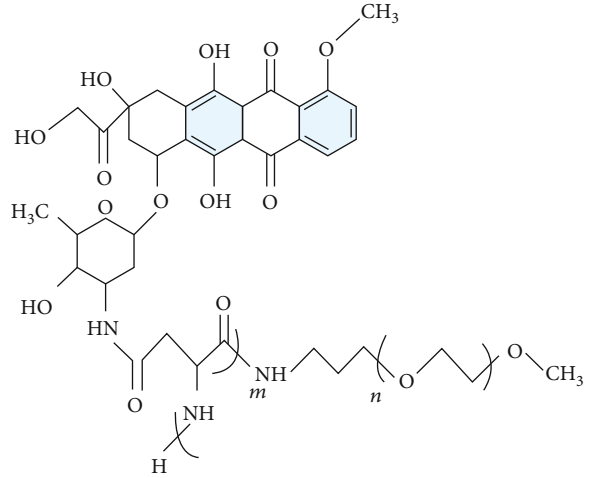
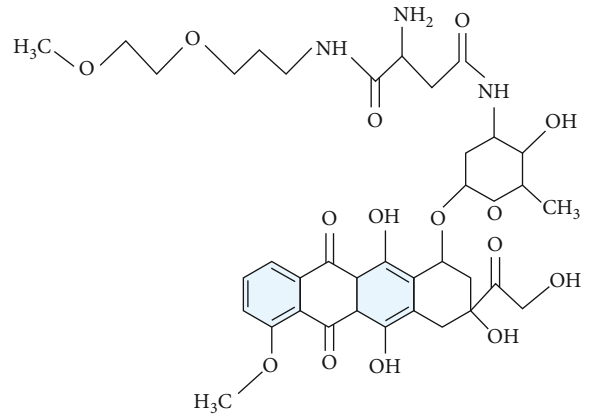
Chemotherapy is sometimes confused with the use of anticancer medications, whereas it refers to the use of chemical compounds to cure cancer in general. Using multicriteria decision-making techniques such as TOPSIS and SAW, this research looked at the behaviors of some drug structures such as anticancer drug SP[n]. This is the first research work to rank several drug structures with the help of certain MCDM techniques. TOPSIS is a ranking method that examines decision-making problems quantitatively and qualitatively. It provides the most accurate and timely solutions to our real-world problems than any other MCDM technique. Furthermore, the simplicity, logic, high processing efficiency, and capacity to quantify relative performance for each choice in a simple mathematical form are also advantages of this technique. On the other hand, one of the most basic and widely used weighted average approaches is the simple additive weighting method. This approach has the advantage of being a proportionate linear translation of the original data, which preserves the relative order of the variables. The SAW method demands normalizing the decision matrix to a scale that is comparable to all other ratings currently available.

2. Preliminaries

This research paper has considered finite graphs without loops and edges [6]. Let us consider a simple graph $G(p, q)$ with vertex set $V(G) = \{v'_1, v'_2, v'_3, \dots, v'_n\}$ and edge set $E(G)$ with $|V(G)| = q$, $|E(G)| = p$. The number of edges connected to vertex $p \in V(G)$ is called degree and is denoted by $d_G(p)$.

In 1975, the topological connectivity index $RI(G)$ of a graph G defined as the sum of weights was proposed by Randić [7], i.e.,

$$RI(G) = \sum_{u' v' \in E(G)} \frac{1}{\sqrt{d_G(u') d_G(v')}}. \quad (1)$$

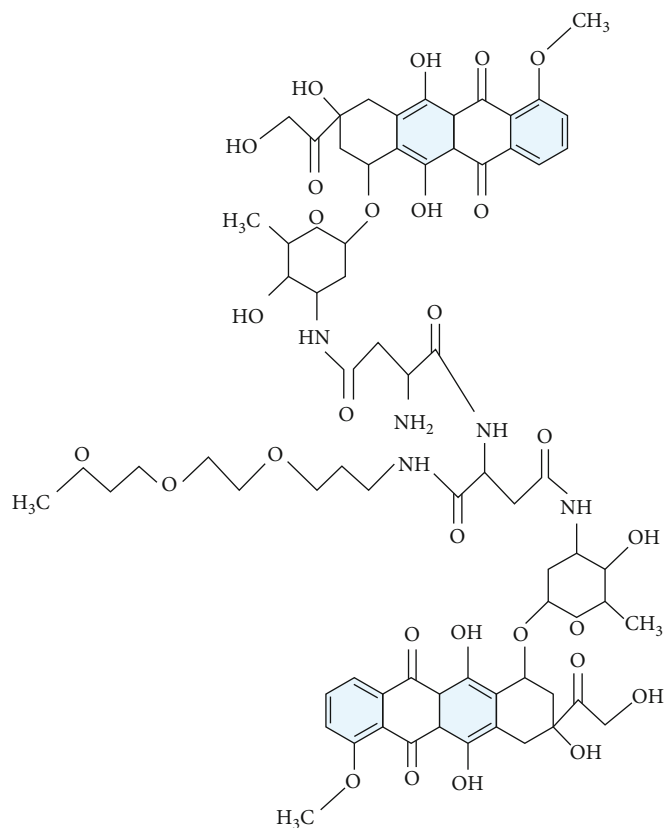
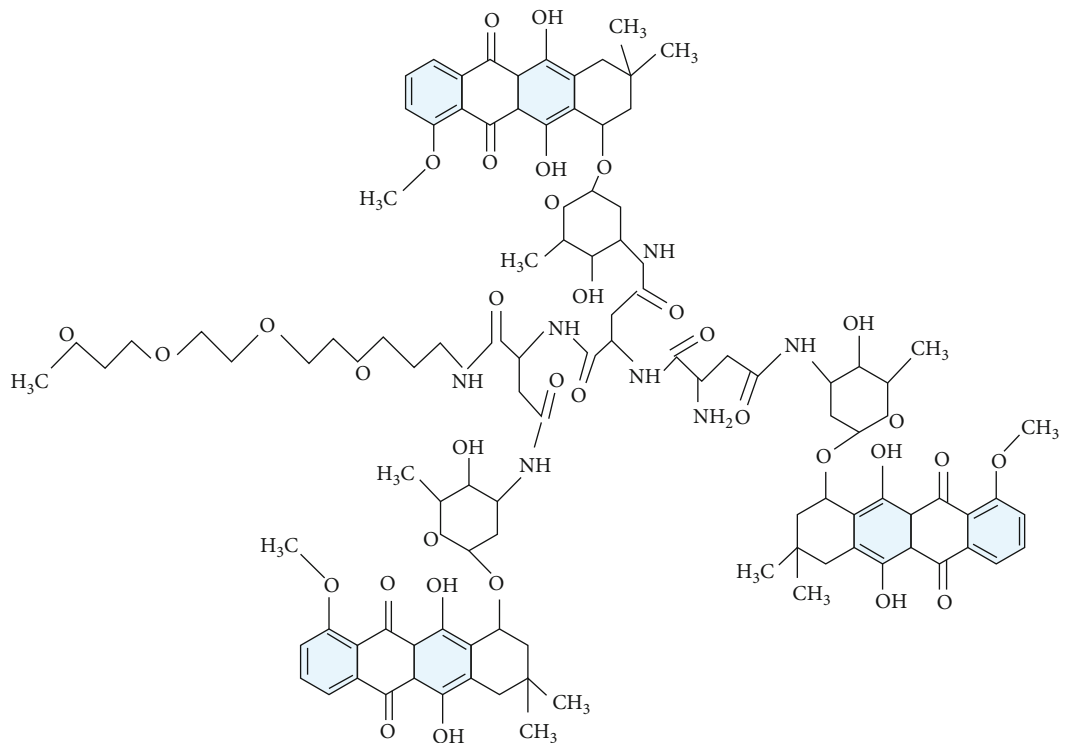
FIGURE 2: Chemical graph of $SP[n]$.FIGURE 3: Chemical graph of $SP[n]$ for $n = 1$.

This index was originally known as the “branching index” or “molecular connectivity index,” and it was found to be useful in determining the level of branching. The Randić index is the name given to this parameter nowadays [8, 9]. Bolllobás and Erdős [10] expanded this index in 1998 by substituting any real number for $-1/2$ to produce the general Randić index RI_α . Thus,

$$RI(G) = \sum_{u' v' \in E(G)} \left(d_G(u') d_G(v') \right)^\alpha. \quad (2)$$

Randić has demonstrated a link between the Randić index and a variety of physicochemical properties [11, 12]. Recently, Dvořák et al. [13] have shown if we have $RI(G) \geq rad(G)/2$, where $rad(G)$ is the radius of G . The main point of their work was to introduce a new index, $RI'(G)$, which was defined as

$$RI'(G) = \sum_{u' v' \in E(G)} \frac{1}{\max \{ d_G(u'), d_G(v') \}}. \quad (3)$$

FIGURE 4: Chemical graph of $\text{SP}[n]$ for $n = 2$.FIGURE 5: Chemical graph of $\text{SP}[n]$ for $n = 3$.

Using this index, Cygan et al. [14] showed that, for any connected graph G of maximum degree at most four that is not a path with an even number of vertices, $(G) \geq \text{rad}(G)$. Consequently, they resolve the conjecture $\text{RI}(G) \geq \text{rad}(G) - 1$ specified by Zhang et al. [15]. They demonstrated that the inequality holds for all connected chemical graphs G , $\text{RI}'(G) \geq \text{rad}(G) - 1/2$ holds.

Furtula et al. [16] recently suggested the enhanced Zagreb index (AZI), a new topological measure based by the ABC index defined as

$$\text{AZI}(G) = \sum_{u'v' \in E(G)} \left(\frac{d(u') + d(v')}{d(u') + d(v') - 2} \right)^3, \quad (4)$$

whose predictive power exceeds that of the ABC index. He revealed that the AZI is a useful predictor of the heat of formation in heptanes and octanes [17]. It is possible to conclude that only this index passed the tests used in this investigation. As a result, when creating quantitative structure–property relationships, this index should be used [18]. Gao et al. [19] defined the forgotten topological index (or, F-index) which is stated as

$$\text{FI}(G) = \sum_{u'v' \in E(G)} \left(d(u')^2 + d(v')^2 \right). \quad (5)$$

De et al. [20] presented some basic properties of the forgotten topological index and demonstrated how this index can improve the Zagreb index's physical-chemical applicability.

3. Drug Structures

In this research paper, we consider several molecular structures of drugs along with their physicochemical properties, i.e., molecular weight, melting point, boiling point, complexity, and density. Disaccharide, its basic structure, has a high energy stability [21]. As a fast-developing platform for targeting CD44-overexpressing cells, HA is a promising cancer treatment [22]. HA works well as a drug transporter and a drug target. Increased water solubility and activity preservation are the great attributes of HA-PTX conjugates; more importantly, they could be applied as targeted drug delivery to boost antitumor efficacy [23]. Figure 1 depicts the structure of hyaluronic acid-paclitaxel conjugates.

The Dox-loaded micelle containing poly-(ethylene glycol)-poly(aspirate) PEG-PAsp block copolymer with chemically conjugated Dox (SP[n]) is depicted in Figure 2.

According to Nishiyama and Kataoka [24], it is a well-known smart polymer family that is used as an anthracycline anticancer antibiotic and is used to treat a variety of cancers. As a result, it possesses strong anticancer properties and is widely utilized in pharmaceuticals. The integer number n is the step of growth in this form of polymer, as seen in Figure 2.

When $n = 1, 2, 3$ (see Figures 3–5, respectively).

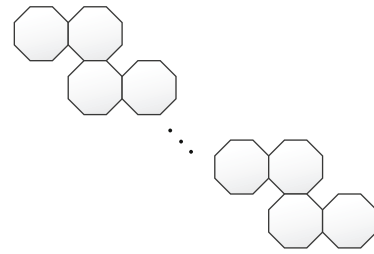


FIGURE 6: The zig-zag chain of 8-cycle Z_n .

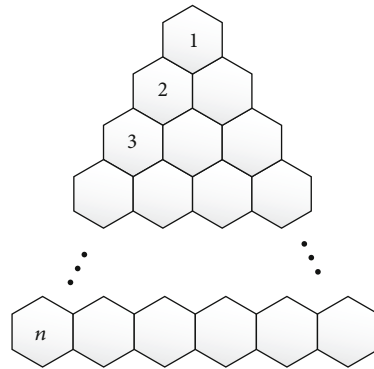


FIGURE 7: Molecular graph of triangular benzenoid T_n .

A polyomino system is a finite 2-connected plane system in which each internal face (also known as a cell) is enclosed by a one-length regular square [25, 26], which contains applications of polyomino systems to crystal physics. A polyomino chain is a polyomino system with a path as its inner dual graph (see Figure 6). It will be denoted by Z_n .

Now, look at the graph of triangular benzenoids T_n , where n is the number of hexagonal structures in the base graph. Figure 7 clearly shows that T_n has $1/2n(n+1)$ hexagons [27]. It is crucial in pharmacy drug design and a variety of other applications.

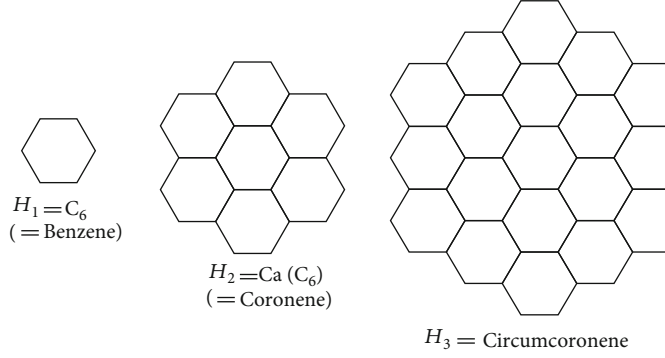
We derive the circumcoronene series of benzenoid after generalizing benzene molecules [28]. Benzene is significant in chemistry because it aids in the production of aromatic compounds. The benzenoid series circumcoronene consists of several copies of benzene C_6 on the perimeter (Figures 8 and 9). One family of benzenoid H_k that arises from the benzene molecule is the circumcoronene series. Coronene H_2 or $\text{Ca}(C_6)$, the first term of the Capra-designed planar benzenoid series $\text{Ca}_n(C_6)$, is a well-known member of this family (C_6).

4. Some Important Results

In this section, we emphasize on calculating the additive degree-based topological indices of the molecular graphs.

- (i) Additive degree-based topological invariants of conjugated Dox SP[n]

Let G be the graph of Dox-loaded micelle comprising PEG-PAsp block copolymer with chemically conjugated

FIGURE 8: Renowned members of circumcoronene benzenoid series H_k for $k \geq 1$.

Dox ($\text{SP}[n]$). Then, we have

$$\begin{aligned} R_1(G) &= 335n + 15, \\ R_{-1}(G) &= 10.611n + 1.333, \\ R_{1/2}(G) &= 131.6286n + 8.69677, \\ AZ(G) &= 444 \cdot 8193n + 19.375, \\ F(G) &= 744n + 34. \end{aligned} \quad (6)$$

From [6], the molecular graph of ($\text{SP}[n]$) contains $49n + 1$ vertices and $54n + 5$ edges.

- (ii) Additive degree-based topological invariants of hyaluronic acid-paclitaxel conjugates G_n

Let G be graph of hyaluronic acid-paclitaxel conjugates G_n . Then, we have

$$\begin{aligned} R_1(G) &= 629n - 11, \\ R_{-1}(G) &= 19.2278n - 0.0278, \\ R_{1/2}(G) &= 243.1083n - 3.4494, \\ AZ(G) &= 822.5972n - 11.3906, \\ F(G) &= 1404n + 23. \end{aligned} \quad (7)$$

From [21], the molecular graph of (G_n) contains $87n$ vertices and $96n$ edges.

- (iii) Additive degree-based topological invariants of polyomino chain of n -cycle Z_n

Let G be graph of polyomino chain of n -cycle Z_n . Then, we have

$$\begin{aligned} RI_1(G) &= 168n - 2, \\ RI_{-1}(G) &= 5.2222n + 0.7778, \\ RI_{1/2}(G) &= 67.5959n + 2, \\ AZI(G) &= 251.125n + 9.2187, \\ FI(G) &= 344n - 4. \end{aligned} \quad (8)$$

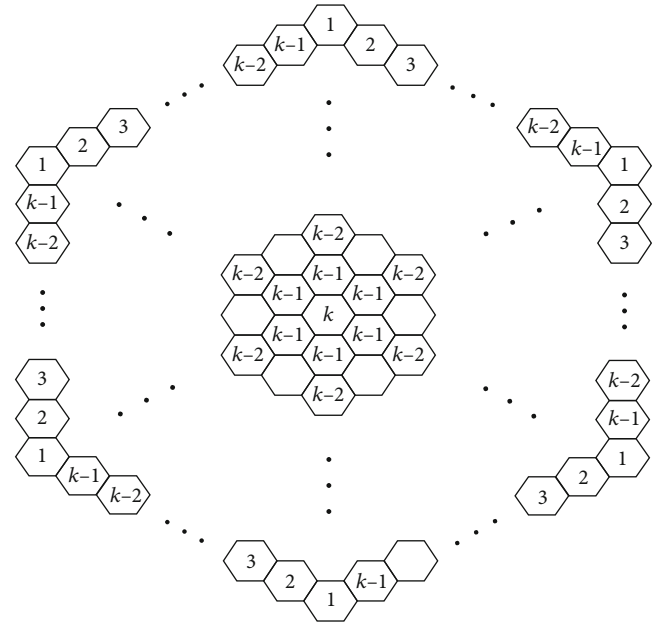
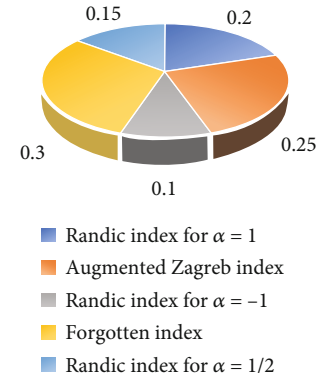
FIGURE 9: The molecular graph of H_k for $k \geq 1$.

FIGURE 10: Allocation of weights

Some of the topological invariants named as I and V have been taken from [29]; the molecular graph of (Z_n) contains $24n + 2$ vertices and $28n + 2$ edges.

- (iv) Additive degree-based topological invariants of circumcoronene series of benzenoid H_k , $k \geq 1$

TABLE 1: Attributes and alternatives.

Alternative	Randić index ($\alpha = 1$)	Augmented Zagreb index	Randić index ($\alpha = -1$)	Forgotten topological index	Randić index ($\alpha = 1/2$)
Hyaluronic acid-paclitaxel conjugates G_1	618	811.2026	19.25	1381	239.6589
Anticancer drug SP[1]	350	464.1943	11.94	778	140.3254
Polyomino chain of n -cycle Z_2	334	511.4687	11.22	684	137.1918
Circumcoronene benzenoid series H_3	546	749.7187	10.17	1173	196.7877
Triangular benzenoid T_6	564	718.4062	12.33	1116	212.2270

TABLE 2: Decision matrix D_{ij} .

Alternatives	RI ₁ (G)	AZI(G)	RI ₋₁ (G)	FI(G)	RI _{1/2} (G)
G_1	618	811.2026	19.25	1381	239.6589
SP[1]	350	464.1943	11.94	778	140.3254
Z_2	334	511.4687	11.22	684	137.1918
H_3	546	749.7187	10.17	1173	196.7877
T_6	564	718.4062	12.33	1116	212.2270

Let G be graph of circumcoronene series of benzenoid H_k , $k \geq 1$. Then, we have

$$\begin{aligned} RI_1(G) &= 81k^2 - 63k + 6, \\ RI_{-1}(G) &= k^2 + 0.333k + 0.1667, \\ RI_{1/2}(G) &= 27k^2 - 15.6061k + 0.60612, \\ AZI(G) &= 102.5156k^2 - 74.8593k + 20.3437, \\ FI(G) &= 162k^2 - 114k. \end{aligned} \quad (9)$$

From [29], the molecular graph of H_k , $k \geq 1$ contains $6k^2 + 6k - 6$ vertices and $9k^2 - 3k$ edges.

(v) Additive degree-based topological indices of triangular benzenoid T_n

Let G be graph of triangular benzenoid T_n . Then, we have

$$\begin{aligned} RI_1(G) &= 9n^2 + 45n - 30, \\ RI_{-1}(G) &= 0.25n^2 + 0.4167n + 0.8333, \\ RI_{1/2}(G) &= 3.6742n^2 - 14.3257n - 6, \\ AZI(G) &= 12n^2 + 56.3437n - 20.3437, \\ FI(G) &= 19.5n^2 + 88.5n - 60. \end{aligned} \quad (10)$$

From [29], the molecular graph of T_n contains $n^2 + 4n + 1$ vertices and $((3/2)3/2n^2) + (9/2)$ edges.

The objectives of this paper are to give behavioral analysis of chemical structures of anticancer drug molecules using several topological indices, such as the Randić index and the augmented Zagreb index, as well as the forgotten topological index. We will also present a weighted evaluation of several topological indices in this research endeavor, as chemical

TABLE 3: Normalized decision matrix H_{ij} .

Alternatives	RI ₁ (G)	AZI(G)	RI ₋₁ (G)	FI(G)	RI _{1/2} (G)
G_1	0.2562	0.2492	0.2965	0.2568	0.2587
SP[1]	0.1451	0.1426	0.1839	0.1515	0.1515
Z_2	0.1284	0.1571	0.1728	0.1332	0.1481
H_3	0.2263	0.2303	0.1566	0.2285	0.2124
T_6	0.2338	0.2208	0.1899	0.2174	0.2291

TABLE 4: Weighted normalized decision matrix X_{ij} .

Alternatives	RI ₁ (G)	AZI(G)	RI ₋₁ (G)	FI(G)	RI _{1/2} (G)
Weight W_j	0.20	0.25	0.10	0.30	0.15
G_1	0.0512	0.0623	0.0296	0.0770	0.0388
SP[1]	0.0290	0.0356	0.0184	0.0454	0.0227
Z_2	0.0276	0.0393	0.0172	0.0399	0.0222
H_3	0.0452	0.0575	0.0156	0.0628	0.0318
T_6	0.0467	0.0552	0.0189	0.0652	0.0343

invariants aim to provide a less expensive and more efficient means for scientists and analysts to determine the physical and chemical features of anticancer medications. Two different decision-making techniques will be used to carry out this weighted evaluation. The Approach for Order Preference by Similarity to Ideal Solution (TOPSIS) will be the first technique. This weighted evaluation will be carried out for the ideal solution and the greatest distance from the worst solution. It also tries to use mathematics to assess the accuracy of molecular compound specifications. This method of multicriteria decision-making first appeared in the 1980s (MCDM).

- (i) Allocation of weights: weights show how much of a drug structure should be taken into account. It is beneficial to have a drug structure with a wide range of physical and chemical properties. In that situation, we give them a lot more weight in comparison to the others and the others do as well (see Figure 10). The weight is allocated according the formula mentioned below

$$\sum_{i=1}^j W'_j = 1. \quad (11)$$

TABLE 5: Calculation of the positive ideal solution L^+ and negative ideal solution L^- .

Alternatives	$RI_1(G)$	$AZI(G)$	$RI_{-1}(G)$	$FI(G)$	$RI_{1/2}(G)$
Properties	Molecular weight	Complexities	Density	Boiling point	Melting point
Weight W_j	0.20	0.25	0.10	0.30	0.15
G_1	0.0512	0.0623	0.0296	0.0770	0.0388
SP[1]	0.0290	0.0356	0.0184	0.0454	0.0227
Z_2	0.0276	0.0393	0.0172	0.0399	0.0222
H_3	0.0452	0.0575	0.0156	0.0628	0.0318
T_6	0.0467	0.0552	0.0189	0.0652	0.0343
L^+ (ideal best)	0.0276	0.0356	0.0156	0.0770	0.0222
L^- (ideal worst)	0.0512	0.0623	0.0296	0.0399	0.0388

TABLE 6: Calculate the separation measures P_i^+ and P_i^- .

Alternatives	$RI_1(G)$	$AZI(G)$	$RI_{-1}(G)$	$FI(G)$	$RI_{1/2}(G)$	P_i^+	P_i^-
G_1	0.0512	0.0623	0.0296	0.0770	0.0388	0.0416	0.0370
SP[1]	0.0290	0.0356	0.0184	0.0454	0.0227	0.0317	0.0402
Z_2	0.0276	0.0393	0.0172	0.0399	0.0222	0.0372	0.0369
H_3	0.0452	0.0575	0.0156	0.0628	0.0318	0.0309	0.0335
T_6	0.0467	0.0552	0.0189	0.0652	0.0343	0.0323	0.0290

(ii) A drug's impact refers to whether it has a positive or negative impact. For example, which physiochemical feature is ideal best and which is ideal worst for our drug structure. The data values for a certain factor should be regarded as standard units

(iii) Ideal best and ideal worst: we must first deal with the properties of our concerned drug structures and then correlate the abovementioned attributes with physical properties of every drug in order to determine the ideal best and ideal worst. The molecular weight, density, complexity, boiling point, and melting point are five common properties of drug structures. The solid density of pharmacological substances, from powder to tablet, is an important feature. It enables us to determine which chemicals will sink in a liquid. If the density of the substance is less than the density of the liquid in which it is immersed, it will flow [30]. As a result, low density is optimal for our pharmacological structures. The melting point is a fundamental physical feature that defines the transition in pharmaceutical sciences, chemical, and biological chemistry. In general, melting points with lower melting points are more likely to be absorbed than melting points with higher melting points. Another key attribute employed in the pharmaceutical industry is molecular weight. The degree of crystallinity of the polymer increased as the molecular weight of the polymer decreased [31]. The drug structures have a molecular weight of less than 1000 g/mol; hence, we use low molecu-

lar weight pharmaceuticals. The boiling point of a medicine is one of its most important characteristics [32]. It is for storing and carrying things. We have more storage for our pharmaceuticals if the boiling point is higher. Drug treatment complexity is acknowledged to be a risk factor for administration errors and nonadherence, resulting in increased healthcare expenses [33]

4.1. TOPSIS. Assume that each property is evaluated independently. Comparing the measure of similarity to the ideal alternative could be used to rate compromises [34]. From Table 1, there are m alternatives (drug structures) and n attributes (Randić indices, augmented Zagreb index, and forgotten topological index). In this regard, we attempt to set appropriate weights for the attributes in order to make the best decision and strike a balance between them [35].

Step 1. Selecting the important attributes and constituting the decision matrix based on m alternatives (drug structures) and n attributes (Randić indices, augmented Zagreb Index, and forgotten topological index) in Table 2:

$$D_{ij} = \begin{bmatrix} d_{11} & d_{12} & \cdots & d_{1n} \\ d_{21} & d_{22} & \cdots & d_{2n} \\ \vdots & \vdots & \ddots & \vdots \\ d_{n1} & d_{n2} & \cdots & d_{nn} \end{bmatrix}. \quad (12)$$

Now, we construct our decision matrix D_{ij} , that is

TABLE 7: Computation of relative closeness to the ideal solution O_i^* .

P_i^+	P_i^-	O_i^*
0.0416	0.0370	0.4706
0.0317	0.0402	0.5592
0.0372	0.0369	0.4975
0.0309	0.0335	0.5206
0.0323	0.0290	0.4730

TABLE 8: Rank the alternatives.

Alternatives	O_i^*	Rank
G_1	0.4706	5
SP[1]	0.5592	1
Z_2	0.4975	3
H_3	0.5206	2
T_6	0.4730	4

Step 2. Calculate the normalized decision matrix H_{ij} (Table 3). The normalized value r_{ij} of the i th alternate (drug structure) with respect to the j th attribute (topological indices).

$$H_{ij} = \begin{bmatrix} h_{11} & h_{12} & \cdots & h_{1n} \\ h_{21} & h_{22} & \cdots & h_{2n} \\ \vdots & \vdots & \ddots & \vdots \\ h_{n1} & h_{n2} & \cdots & h_{nn} \end{bmatrix}, \quad (13)$$

where $H_{ij} = d_{ij}/\sqrt{\sum_{i=1}^m d_{ij}^2} \forall j = 1, 2, 3, \dots, n$ and $i = 1, 2, 3, \dots, m$.

Step 3. Calculate the weighted normalized decision matrix X_{ij} shown in Table 4.

The weighted normalized value is $X_{ij} = W_j' \cdot h_{ij} \forall j = 1, 2, 3, \dots, n$, where

$$\sum_{i=1}^j W_j' = 1. \quad (14)$$

Here, we allocate the highest-ranking topological descriptor highest weight. $RI_{-1}(G)$ gives small values of their respective drug structures so that we assign lowest weight (0.10). Similarly, $RI_{1/2}(G)$ has slightly different values from $RI_{-1}(G)$ so we allocate it with little more weight (0.15). Next, if we notice $RI_1(G)$, the values for it are greater than $RI_{1/2}(G)$ so we assign weight (0.20). Lastly, if we see $FI(G)$, that is richest in their values, we give a maximum weight (0.30) to it.

$$W_j' = 0.20, 0.25, 0.10, 0.30, 0.15. \quad (15)$$

TABLE 9: The decision matrix G_{ij} .

Alternatives	$R_1(G)$	AZ(G)	$R_{-1}(G)$	$F(G)$	$R_{1/2}(G)$
G_1	618	811.2026	19.25	1381	239.6589
SP[1]	350	464.1943	11.94	778	140.3254
Z_2	334	511.4687	11.22	684	137.1918
H_3	546	749.7187	10.17	1173	196.7877
T_6	564	718.4062	12.33	1116	212.2270
Best (g_j^+)	334	464.1943	10.17	1381	137.1918
Worst (g_j^-)	618	811.2026	19.25	684	239.6589

TABLE 10: Normalized decision matrix H_{ij} .

Alternatives	$R_1(G)$	AZ(G)	$R_{-1}(G)$	$F(G)$	$R_{1/2}(G)$
Weight W_j	0.20	0.25	0.10	0.30	0.15
G_1	0.540453	0.57223	0.528312	1	0.572446
SP[1]	0.954286	1	0.851759	0.56336	0.977669
Z_2	1	0.907571	0.906417	0.495293	1
H_3	0.611722	0.619158	1	0.849385	0.697156
T_6	0.592199	0.646145	0.824818	0.80811	0.646439

TABLE 11: Rank the alternatives.

Alternatives	M_i	Rank
G_1	0.689846	5
SP[1]	0.841691	1
Z_2	0.816123	2
H_3	0.736523	3
T_6	0.701856	4

We can calculate the normalized decision matrix using the formula given below.

$$X_{ij} = \begin{bmatrix} W_1' h_{11} & W_1' h_{11} & \cdots & W_n' h_{1n} \\ W_1' h_{21} & W_2' h_{22} & \cdots & W_n' h_{2n} \\ \vdots & \vdots & \ddots & \vdots \\ W_1' h_{n1} & W_2' h_{n2} & \cdots & W_n' h_{nn} \end{bmatrix}. \quad (16)$$

Step 4. Determine the positive ideal solution L^+ and negative ideal solution L^- (Table 5).

To determine the distance between alternative i and the ideal alternative that is defined as

$$L^+ = \left\{ x_i^+, \dots, x_j^+ \right\} = (\max \text{ (or } \min) X_{ij} | j \in J), \quad (17)$$

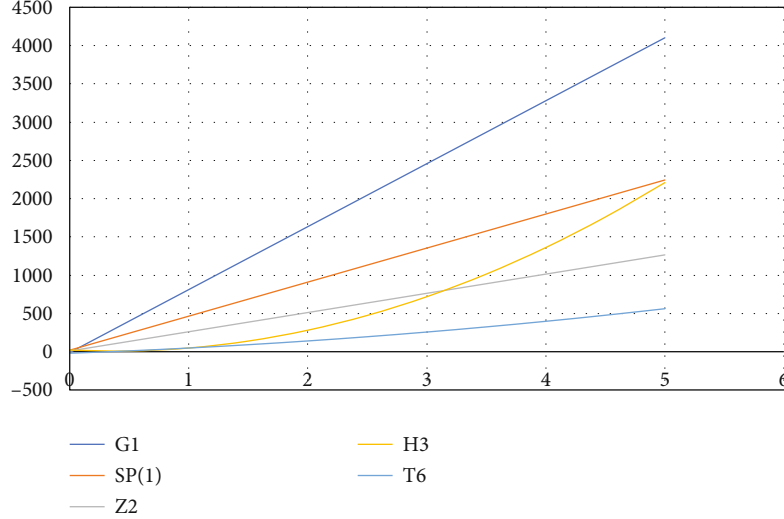


FIGURE 11: Comparison of alternatives using AZI(G).

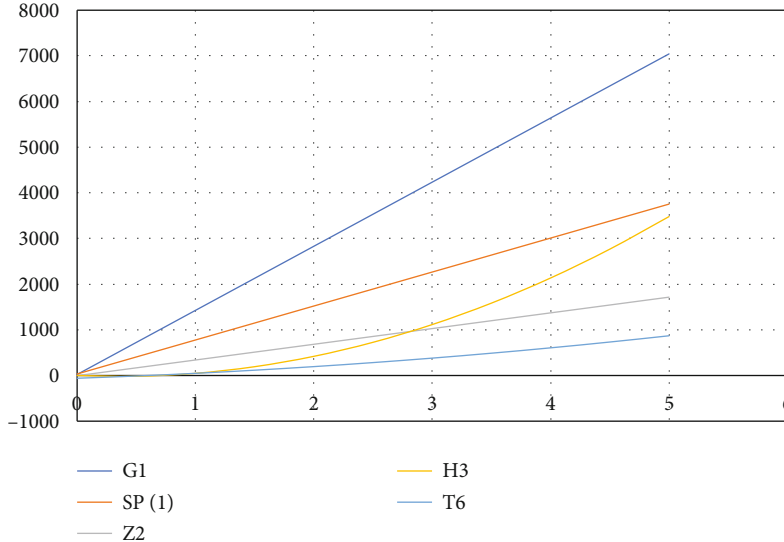


FIGURE 12: Comparison of alternatives using FI(G).

and distance between alternative i and the minimum alternative that is defined as

$$L^- = \left\{ x_i^-, \dots, x_j^- \right\} = (\min \text{ (or max)} X_{ij} | j \in J). \quad (18)$$

Step 5. Compute the separation measure, using the n -dimensional Euclidean distance in Table 6. The separation of each alternative form the ideal solution is given by

$$P_i^+ = \sqrt{\sum_{j=1}^n (X_{ij} - L_j^+)^2}, \quad (19)$$

$$P_i^- = \sqrt{\sum_{j=1}^n (X_{ij} - L_j^-)^2}.$$

Step 6. Compute the relative closeness to the ideal solution (Table 7). The relative closeness of A_i with respect to A is defined as

$$O_i^* = \frac{P_i^-}{P_i^+ + P_i^-}, \quad (20)$$

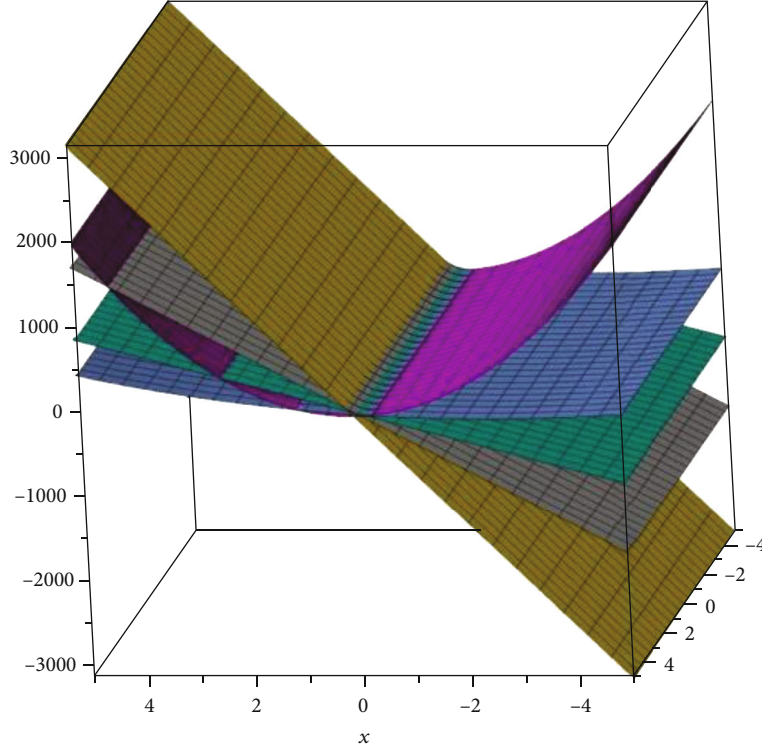
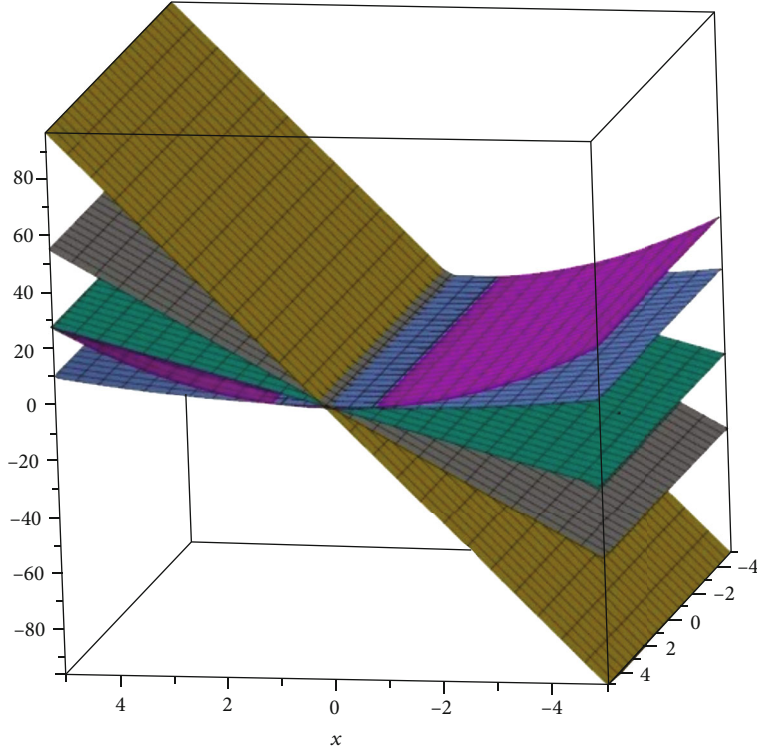
where $0 < O_i^* < 1$, $i = 1, 2, 3, \dots, n$.

It is clear that $O_i^* = 1$ if $L_i = L^+$ and $O_i^* = 0$ if $L_i = L^-$.

Therefore, a preferable option is the one that poses the value closer to 1.

Step 7. Rank the reference order based on the descending order of O_i^* in Table 8.

4.2. SAW. A multicriteria decision-making (MCDM) or multicriteria decision analysis method is the simple additive

FIGURE 13: Comparison of alternatives using $RI_1(G)$.FIGURE 14: Comparison of alternatives using $RI_{-1}(G)$.

weighting method (SAW), which is also known as weighted linear combination or scoring method [36]. This method is comprised on the weighted average. The weighted sum of the performance evaluations for every alternative among all

attributes is determined using the SAW method [37]. There are different m alternatives (drug structures) and n attributes (Randić indices, augmented Zagreb index, and forgotten topological index).

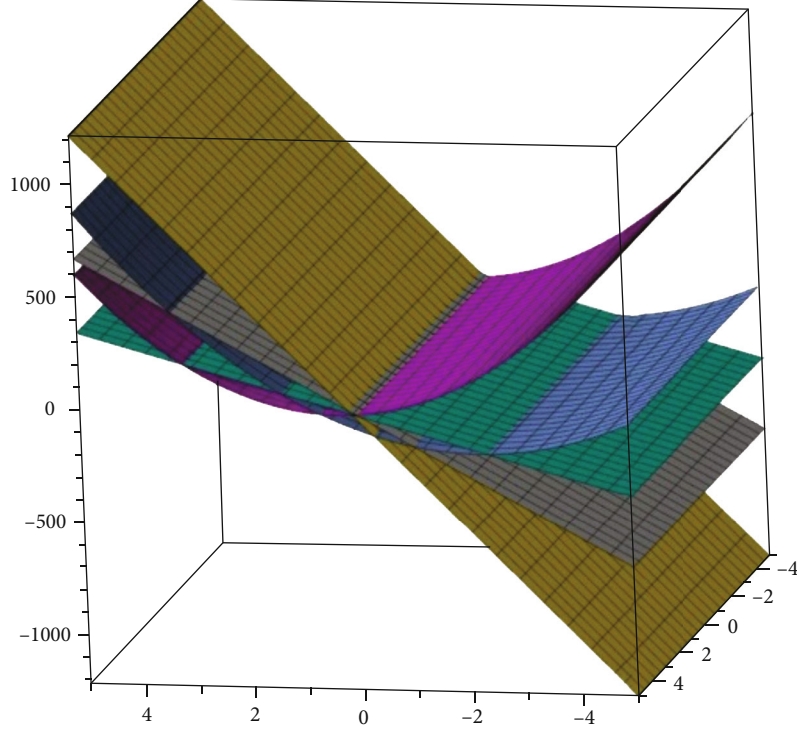
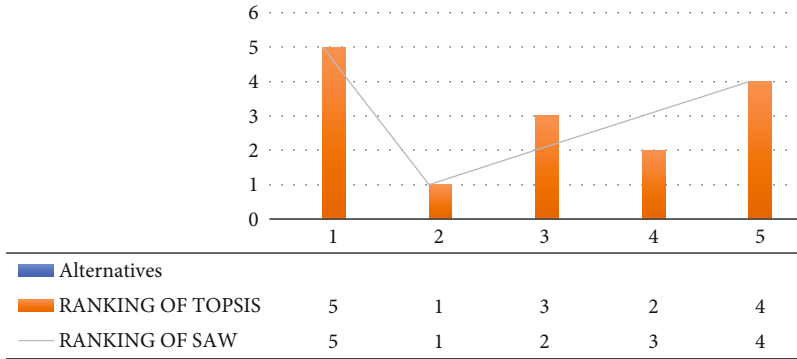
FIGURE 15: Comparison of alternatives using $RI_{1/2}(G)$.

FIGURE 16: Ranking of TOPSIS and SAW.

The SAW method's compromise ranking algorithm consists of the following steps:

Step 1. Constitute the decision matrix of m alternatives and n attributes in Table 9.

$$G_{ij} = \begin{bmatrix} g_{11} & g_{12} & \cdots & g_{1n} \\ g_{21} & g_{22} & \cdots & g_{2n} \\ \vdots & \vdots & \ddots & \vdots \\ g_{n1} & g_{n2} & \cdots & g_{nn} \end{bmatrix}. \quad (21)$$

And determine the best g_j^+ and worst g_j^- values of all the attributes $j = 1, 2, 3, \dots, n$.

Step 2. By using the abovementioned weighted criteria, we calculate the weights. Also, construct a normalized decision matrix H_{ij} according to the formula given below, where m is the alternatives and n is the attributes in Table 10.

$$h_{ij} = \frac{g_{ij}}{\max(g_{ij})}, \quad (22)$$

$$h_{ij} = \frac{\min(g_{ij})}{g_{ij}},$$

where $i = 1, 2, 3, \dots, m$ and $j = 1, 2, 3, \dots, n$.

Step 3. Evaluate each alternative M_i by the following formula (Table 11):

$$M_i = \sum_{j=1}^n W_j h_{ij}, \quad (23)$$

where h_{ij} is the score of i th alternative with respect to the j th attribute and W_j is the weighted criteria of the attributes.

5. Graphical Interpretation of Drug Structures

The two-dimensional and three-dimensional graphical comparisons of the above results are depicted in Figures 11–15, respectively.

5.1. Two-Dimensional Graphs. In both the 2D plots of the drug structures along with the attributes, we have found that G_1 gives us the highest value and T_6 shows the smallest value.

5.2. Three-Dimensional Graphs. These 3D graphs are representing the behavior of the drug structures with attributes $RI_1(G)$, $RI_{-1}(G)$, and $RI_{1/2}(G)$, respectively. Golden color is indicating G_1 drug structure, grey is indicating $SP[1]$, green is indicating Z_2 , Niagara azure is indicating H_3 , and purple is indicating T_6 drug structures. In all the graphs, we have clearly seen that G_1 gives us effective role as a drug structure in these plots.

6. Conclusion

Many drug studies reveal strong inner links between the medications' biological and pharmacological properties and their molecular structures. In this research article, using TOPSIS method, $SP[1]$ is determined to be the most suitable drug structure as it has close distance to the ideal solution. The drug structures are thus ranked as H_3 , Z_2 , T_6 , and lastly G_1 , i.e., $H_3 > Z_2 > T_6 > G_1$. On the other hand, using SAW, we have observed a slightly changed behavior of drugs as Z_2 and H_3 are ranked opposite in their behaviors. In the SAW method, $SP[1]$ is determined to be the highest ranked drug structure. Other structures are ranked as $Z_2 > H_3 > T_6 > G_1$. Moreover, the results are plotted using the MS Excel and MAPLE in Figures 11–15, respectively. These theoretical results might be supportive to comprehend the topology of the aforementioned chemical drug structures. The histogram of the ranking is created through the MS Excel as shown in Figure 16. These theoretical results might be helpful to rank the drug structures via chemical invariants in the field of medicine, chemistry, drug discovery, and mathematical chemistry while evaluating these drugs in future.

Data Availability

The data used to support this work are cited within the text as references.

Conflicts of Interest

The authors declare that they have no conflicts of interest.

Authors' Contributions

This work was equally contributed by all writers.

Acknowledgments

This work was supported by the Deanship of Scientific Research, Vice Presidency for Graduate Studies and Scientific Research, King Faisal University, Saudi Arabia (Grant No. 2715).

References

- [1] G. W. Milne, "Mathematics as a basis for chemistry," *Journal of Chemical Information and Computer Sciences*, vol. 37, no. 4, pp. 639–644, 1997.
- [2] N. Trinajstić, *Chemical Graph Theory*, CRC Press, Boca Raton, FL, 2nd edition, 1992.
- [3] O. Ivanciu, T. Ivanciu, and A. T. Balaban, "Vertex-and edge-weighted molecular graphs and derived structural descriptors," in *Topological Indices and Related Descriptors in QSAR and QSPR*, pp. 169–175, CRC Press, 1999.
- [4] W. Gao, W. Wang, and M. R. Farahani, "Topological indices study of molecular structure in anticancer drugs," *Journal of Chemistry*, vol. 2016, Article ID 3216327, 8 pages, 2016.
- [5] A. R. Katritzky, R. Jain, A. Lomaka, R. Petrukhin, U. Maran, and M. Karelson, "Perspective on the relationship between melting points and chemical structure," *Crystal Growth & Design*, vol. 1, no. 4, pp. 261–265, 2001.
- [6] Z. Shao, A. Jahanbani, and S. M. Sheikholeslami, "Multiplicative topological indices of molecular structure in anticancer drugs," *Polycyclic Aromatic Compounds*, vol. 42, no. 2, pp. 475–488, 2022.
- [7] M. Randic, "Characterization of molecular branching," *Journal of the American Chemical Society*, vol. 97, no. 23, pp. 6609–6615, 1975.
- [8] X. Zhang, A. Rauf, M. Ishtiaq, M. K. Siddiqui, and M. H. Muhammad, "On degree based topological properties of two carbon nanotubes," *Polycyclic Aromatic Compounds*, vol. 42, no. 3, pp. 866–884, 2022.
- [9] X. Zhang, M. K. Siddiqui, S. Javed, L. Sherin, F. Kausar, and M. H. Muhammad, "Physical analysis of heat for formation and entropy of ceria oxide using topological indices," *Combinatorial Chemistry & High Throughput Screening*, vol. 25, no. 3, pp. 441–450, 2022.
- [10] B. Bollobás and P. Erdős, "Graphs of extremal weights," *Ars combinatoria*, vol. 50, pp. 225–233, 1998, <https://digitalcommons.memphis.edu/facpubs/4851>.
- [11] X. Li and Y. Shi, "A survey on the Randic index," *Match-Communications in Mathematical and Computer Chemistry*, vol. 59, no. 1, pp. 127–156, 2008.
- [12] P. Hansen and H. Mélot, "Variable neighborhood search for extremal graphs. 6. Analyzing bounds for the connectivity index," *Journal of Chemical Information and Computer Sciences*, vol. 43, no. 1, pp. 1–14, 2003.

- [13] Z. Dvořák, B. Lidický, and R. Škrekovski, “Randić index and the diameter of a graph,” *European Journal of Combinatorics*, vol. 32, no. 3, pp. 434–442, 2011.
- [14] M. Cygan, M. Pilipczuk, and R. Škrekovski, “On the inequality between radius and Randic index for graphs,” *Match-Communications in Mathematical and Computer Chemistry*, vol. 67, no. 2, pp. 451–465, 2012.
- [15] X. Zhang, X. Wu, S. Akhter, M. K. Jamil, J. B. Liu, and M. Farahani, “Edge-version atom-bond connectivity and geometric arithmetic indices of generalized bridge molecular graphs,” *Symmetry*, vol. 10, no. 12, pp. 751–786, 2018.
- [16] B. Furtula, A. Graovac, and D. Vukičević, “Atom-bond connectivity index of trees,” *Discrete Applied Mathematics*, vol. 157, no. 13, pp. 2828–2835, 2009.
- [17] X. Zhang, H. Jiang, J. B. Liu, and Z. Shao, “The cartesian product and join graphs on edge-version atom-bond connectivity and geometric arithmetic indices,” *Molecules*, vol. 23, no. 7, p. 1731, 2018.
- [18] I. Gutman and J. Tošović, “Testing the quality of molecular structure descriptors. Vertex-degree-based topological indices,” *Journal of the Serbian Chemical Society*, vol. 78, no. 6, pp. 805–810, 2013.
- [19] W. Gao, M. R. Farahani, and L. Shi, “Forgotten topological index of some drug structures,” *Acta medica mediterranea*, vol. 32, no. 1, pp. 579–585, 2016.
- [20] N. De, S. M. A. Nayem, and A. Pal, “F-index of some graph operations,” *Discrete mathematics, algorithms and applications*, vol. 8, no. 2, article 1650025, 2016.
- [21] L. Zheng, Y. Wang, and W. Gao, “Topological indices of hyaluronic acid-paclitaxel conjugates’ molecular structure in cancer treatment,” *Open Chemistry*, vol. 17, no. 1, pp. 81–87, 2019.
- [22] A. Mráček, J. Varhaníková, M. Lehocký, L. Gründelová, A. Pokopcová, and V. Velebný, “The influence of Hofmeister series ions on Hyaluronan swelling and viscosity,” *Molecules*, vol. 13, no. 5, pp. 1025–1034, 2008.
- [23] F. Dosio, S. Arpicco, B. Stella, and E. Fattal, “Hyaluronic acid for anticancer drug and nucleic acid delivery,” *Advanced Drug Delivery Reviews*, vol. 97, pp. 204–236, 2016.
- [24] N. Nishiyama and K. Kataoka, “Polymeric micelle drug carrier systems: PEG-PAsp (Dox) and second generation of micellar drugs,” in *Polymer Drugs in the Clinical Stage*, Advances in Experimental Medicine and Biology, H. Maeda, A. Kabanov, K. Kataoka, and T. Okano, Eds., pp. 155–177, Springer, Boston, MA, 2004.
- [25] J. Rada, “The linear chain as an extremal value of VDB topological indices of polyomino chains,” *Applied Mathematical Sciences*, vol. 8, pp. 5133–5143, 2014.
- [26] P. John, H. Sachs, and H. Zernitz, “Counting perfect matchings in polyominoes with an application to the dimer problem,” *Applicationes Mathematicae*, vol. 19, no. 3-4, pp. 465–477, 1987.
- [27] J. R. Dias, “Correlations and topology of triangular benzenoid hydrocarbons: a comparative study of two series representing the least and most stable benzenoid hydrocarbons,” *Journal of Physical Organic Chemistry*, vol. 15, no. 2, pp. 94–102, 2002.
- [28] M. R. Farahani, “Computing edge-PI index and vertex-PI index of circumcoronene series of benzenoid H_k by use of cut method,” *International Journal of Mathematical Modeling and Applied Computing*, vol. 1, no. 6, pp. 41–50, 2013.
- [29] M. Cancan, S. Mondal, N. De, and A. Pal, “Multiplicative degree based topological indices of some chemical structures in drug,” *Proyecciones (Antofagasta)*, vol. 39, no. 5, pp. 1347–1364, 2020.
- [30] Q. Du, Y. Li, and L. Pan, “Wheelchair size and material application in human-machine system model,” *Applied Mathematics and Nonlinear Sciences*, vol. 6, no. 2, pp. 7–18, 2021.
- [31] R. Bu, C. Qu, and Y. G. Sánchez, “Nonlinear mathematical modelling of bone damage and remodelling behaviour in human femur,” *Applied Mathematics and Nonlinear Sciences*, vol. 6, no. 2, pp. 53–64, 2021.
- [32] M. Du, Y. Liu, and L. Li, “An empirical investigation of physical literacy-based adolescent health promotion,” *Applied Mathematics and Nonlinear Sciences*, vol. 6, no. 2, pp. 133–146, 2021.
- [33] L. Sen, Z. Yang, Z. Caihong, and W. Chengliang, “A comprehensive evaluation of county economies in the Beijing-Tianjin-Hebei region based on entropy TOPSIS analysis,” *Applied Mathematics and Nonlinear Sciences*, vol. 6, no. 2, pp. 499–516, 2021.
- [34] K. Naeem, M. Riaz, and F. Karaaslan, “A mathematical approach to medical diagnosis via Pythagorean fuzzy soft TOPSIS, VIKOR and generalized aggregation operators,” *Complex & Intelligent Systems*, vol. 7, no. 5, pp. 2783–2795, 2021.
- [35] E. Roghanian and Z. Shakeri Kebria, “The combination of TOPSIS method and Dijkstra’s algorithm in multi-attribute routing,” *Scientia Iranica*, vol. 24, no. 5, pp. 2540–2549, 2017.
- [36] Ž. Stević, E. Durmić, M. Gajić, D. Pamučar, and A. Puška, “A novel multi-criteria decision-making model: interval rough SAW method for sustainable supplier selection,” *Information*, vol. 10, no. 10, pp. 292–299, 2019.
- [37] Y. Irawan, “Decision support system for employee bonus determination with web-based simple additive weighting (SAW) method in PT. Mayatama Solusindo,” *Journal of Applied Engineering and Technological Science (JAETS)*, vol. 2, no. 1, pp. 7–13, 2020.